Twisting Light by Nonlinear Photonic Crystals

Noa Voloch Bloch,[1] Keren Shemer,[1] Asia Shapira,[1] Roy Shiloh,[1] Irit Juwiler,[2] and Ady Arie[1,*]

[1]*Department of Physical Electronics, Fleischman Faculty of Engineering, Tel Aviv University, Tel Aviv 69978, Israel*
[2]*Department of Electrical and Electronics Engineering, Sami Shamoon College of Engineering, Ashdod 77245, Israel*

(Received 8 January 2012; published 8 June 2012)

We report the observation of nonlinear interactions in quadratic nonlinear crystals having a geometrically twisted susceptibility pattern. The *quasi-angular-momentum* of these crystals is imprinted on the interacting photons during the nonlinear process so that the total angular momentum is conserved. These crystals affect three basic physical quantities of the output photons: energy, translational momentum, and angular momentum. Here we study the case of second-order harmonic vortex beams, generated from a Gaussian pump beam. These crystals can be used to produce multidimensional entanglement of photons by angular momentum states or for shaping the vortex's structure and polarization.

DOI: 10.1103/PhysRevLett.108.233902 PACS numbers: 42.65.Ky, 42.25.Fx, 42.40.Jv

Introduction.—A fundamental property of light is its ability to rotate when traveling in space. The common form of such rotation is the polarization rotation, or spin angular momentum. Photons of light carrying spin angular momentum have two possible values of quantized angular momentum, $\pm\hbar$. Only 20 years ago Allen *et al.* [1] recognized that light has another form of angular momentum originating from its helical wavefront structure, known as orbital angular momentum (OAM). Optical vortex beams have a phase singularity at the center of the optical axis and a phase winding factor of $e^{il\phi}$. The OAM of such beams can have any positive or negative integer multiple of $\hbar$ [1–4]. Optical vortices have been studied in various research fields, e.g., rotating optical tweezers, transferring their angular momentum to microparticles and causing them to spin around the beam's axis [5]. Since the state of photons with angular momentum lie in a multidimensional Hilbert space, entanglement of angular momentum can be used for quantum computation [6]. One of the latest findings showed that light traveling around a Kerr black hole [7] is imprinted with angular momentum. Even electron beams exhibited a phase singularity when they were diffracted from a structure with a topological dislocation [8].

Optical vortices have also been explored in various nonlinear processes [9–11], but the angular momentum of the generated photons was determined by the OAM of the input waves alone. However, to the best of our knowledge, none of the nonlinear conversion processes studied before took place in a twisted nonlinear medium, where the quadratic susceptibility structure has a topological charge of its own, or *quasi-angular-momentum*. We found experimentally that photons interacting in a twisted nonlinear photonic crystal (NPC) are imprinted with the crystal's topological charge in order to conserve the total angular momentum, i.e., the OAM of the generated waves depends not only on the OAM of the input waves but also on the crystal's topological charge. We formulated a general conservation law for the angular momentum in nonlinear conversion processes which includes the *quasi-angular-momentum* of the structure $l_c\hbar$. To prove this, we studied the nonlinear second harmonic (SH) frequency conversion process within various twisted NPCs, using a Gaussian TEM_{00} pump input beam having no angular momentum, as shown in Fig. 1.

The most wide-spread technique to fabricate NPCs is by electric field poling in ferroelectric materials [12]. In the poling process the nonlinear coefficient is permanently reversed by applying a high voltage pulse through a patterned electrode. This is essentially a planar technology that enables the modulation of the nonlinear coefficient in only two dimensions. Quasi-phase-matching is done in

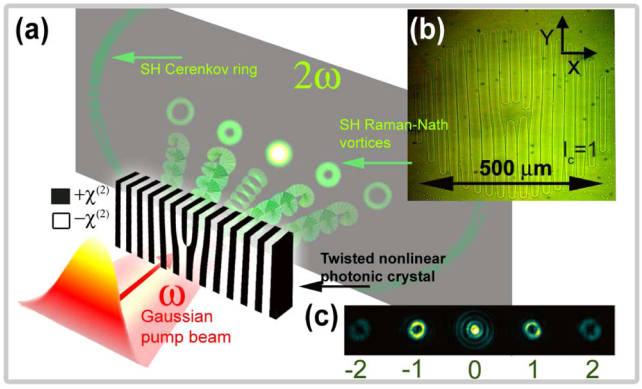

FIG. 1 (color online). (a) Experiment description: A Gaussian pump beam enters transversely into a twisted nonlinear photonic crystal. The pump beam has no angular momentum. SH vortex beams are nonlinearly generated at the nonlinear Raman-Nath diffraction orders. (b) Microscope image of the twisted nonlinear photonic crystal. The nonlinear modulation is revealed by selective etching of the crystal surface. (c) Experimental observation of second-order harmonic nonlinear vortices from a fork shaped structure of $l_c = 1$. The numbers indicate the OAM value of each vortex.

two ways: longitudinally [13–15] or the transverse [16–19] way (see Supplementary Information).

Nonlinear generation of vortex beams.—Generating vortex beams from a Gaussian TEM_{00} beam by a nonlinear process was first suggested in Ref. [20]. The theoretical NPCs presented there were based on a 3D modulation of the nonlinear susceptibility. Recently, it was also proposed to use these 3D type structures to manipulate vortex beams through the Pockels electro-optic effect [21]. Unfortunately, these structures have not yet been realized experimentally, since they rely on 3D modulation of the nonlinear (or electro-optical) coefficient—a very challenging technology unavailable in most of the relevant materials.

Here we show that 3D modulation is not needed. Optical vortices can be generated from an NPC—fabricated by the standard (planar) poling technique—by utilizing the transverse nonlinear diffraction effects. We fabricated twisted NPCs with a quadratic nonlinear coefficient having either a fork or a spiral pattern. We illuminated the twisted NPCs transversely with a Gaussian pump beam as shown in Fig. 2(c). In this way, we nonlinearly generated SH optical vortices, which were obtained at Raman-Nath nonlinear diffraction orders. Conservation of OAM is maintained due to the crystal's quasi-angular-momentum. The SH angular momentum is identified as the dark core (caused by destructive interference) imprinted on each diffracted order. The topological charge of the vortices results from the topological charge of the twisted nonlinear photonic crystal itself. The resulting SH radiation from a fork-shaped structure is a set of vortices with increasing radii, owing to the increased topological charge of each diffracted order.

Conservation of OAM in twisted NPCs.—The general binary function that represents the pattern of the twisted NPC's second-order nonlinear susceptibility is:

$$\chi^{(2)}(\mathbf{r}, \phi) = d_{ij}\mathrm{sgn}\{\cos[2\pi f(\mathbf{r}, \phi) + l_c\phi]\}, \qquad (1)$$

where d_{ij} is an element of the quadratic susceptibility $\chi^{(2)}$ tensor, $\mathbf{r} = x\hat{\mathbf{x}} + y\hat{\mathbf{y}}$, $\phi = \tan^{-1}(y/x)$ is the azimuthal angle and l_c is the topological charge of the crystal which can have an integer or fractional value. $f(\mathbf{r}, \phi)$ can be any 1D or 2D function such as $f(\mathbf{r}, \phi) = |\mathbf{r}|\cos(\phi)/\Lambda$ for a fork shaped structure, or $f(\mathbf{r}, \phi) = |\mathbf{r}|/\Lambda$ for a spiral structure, where Λ, in both cases, is the poling period. This binary modulation function can be expanded to a series of oscillating terms usually with a dominant first-order term equal to $F_1 \exp[i2\pi f(\mathbf{r}, \phi) + il_c\phi]$, where F_1 is the Fourier coefficient. We consider a transverse phase matching configuration where the input pump wave propagates in the $\hat{\mathbf{z}}$ direction and is ordinary polarized in the $\hat{\mathbf{y}}$ direction. The highest contribution in small diffraction angles is from the d_{yyy} of $\chi^{(2)}$. We consider a pump and an SH wave with arbitrary envelopes A_1, A_2: $E_1(\mathbf{r}, \phi, z) = A_1 e^{il_1\phi + ik_1 z}$, $E_2(\mathbf{r}, \phi, z) = A_2 e^{i\mathbf{k}_{2_t}\cdot\mathbf{r} + ik_{2_z}z}$, where l_1 is the topological charge of the pump wave. The SH wave is propagating at an arbitrary angle, therefore its wave vector has longitudinal and transverse components: k_{2_z}, $\mathbf{k}_{2_t}$. Assuming that the pump is undepleted and that the fields' envelopes vary slowly, the evolution of the SH wave is given by

$$\frac{dA_2}{dz} = \kappa A_1^2 e^{i(2l_1 + l_c)\phi} e^{i(2k_1 - k_{2_z})z} e^{i2\pi f(\mathbf{r},\phi) - i\mathbf{k}_{2_t}\cdot\mathbf{r}}, \qquad (2)$$

where κ is the nonlinear coupling coefficient. Here we can see the separate contributions of the topological charge (the left term), the longitudinal phase mismatch (Čerenkov diffraction, the middle term) and the transverse phase mismatch (Raman-Nath diffraction, the right term). If we select a first-order nonlinear Raman-Nath diffraction component so that the transverse phase matching condition is satisfied, the right exponent can be approximated as 1. This occurs, for example, if we have a periodic modulation in the $\hat{\mathbf{x}}$ direction with a period Λ_x, i.e.,

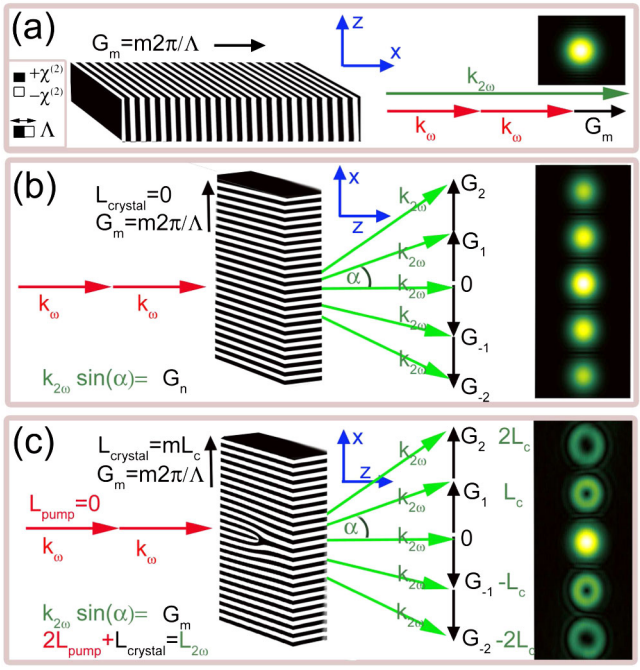

FIG. 2 (color online). Conservation laws of translational momentum and angular momentum in quasi-phase-matched NPCs. Red [medium gray], green [light gray] and black arrows indicate the wave vectors of the pump beam, the SH radiation, and the reciprocal lattice vector, respectively. The right inset on each panel represents the far-field SH intensity. (a) The standard longitudinal collinear quasi-phase-matching scheme. (b) Conservation of the translational momentum in the transverse direction yields the Raman-Nath diffraction pattern [16]. (c) The case studied here: transverse nonlinear scattering from a fork shaped nonlinear photonic crystal, having a quasi-angular-momentum. SH vortices are generated from a Gaussian pump beam with no angular momentum. The angular momentum can be identified as the dark core imprinted on different diffraction orders due to destructive interference at the center of each order. [Note that the Čerenkov ring is not sketched in panels (b) and (c).]

$f(\mathbf{r}, \phi) = |\mathbf{r}|\cos(\phi)/\Lambda_x = x/\Lambda_x$, and a transverse term of the SH wave that satisfies $\mathbf{k}_{2_t} = 2\pi/\Lambda_x\hat{\mathbf{x}}$. The SH amplitude at the output of the crystal, at the direction that is defined by $\mathbf{k}_2$ becomes, in this case

$$A_2 \approx \kappa \frac{A_1^2 e^{i(2k_1 - k_{2_z})L}}{i(2k_1 - k_{2_z})L} e^{i(2l_1 + l_c)\phi} = A_{2\check{C}} e^{i(2l_1 + l_c)\phi}, \quad (3)$$

where L is the crystal's thickness. $A_{2\check{C}}$ is maximized in the case of longitudinal phase matching. Regardless of $A_{2\check{C}}$'s value, we still get a phase term of a vortex beam. We only need to avoid a crystal thickness that nulls the amplitude of A_2 [22]. A general conservation law for the OAM in an SH generation process results from Eq. (3): $l_2 = 2l_1 + l_c$, where l_2 is the OAM of the SH wave. This conservation law can be generalized to all nonlinear processes. Let us consider first a simple case for which the input pump beam has no OAM, as depicted in Fig. 1. The generated SH wave will have a phase term with azimuthal dependence $\exp(il_c\phi)$, which originates from the nonlinear crystal. This shows that SH vortex beams can be generated from nonvortex pump beams. In the case where the pump beam does have OAM, the topological charge of the generated beam is equal to the sum of twice the charge of the input beam and the charge of the nonlinear crystal. This is in clear contrast to the case of diffraction through a linear phase mask, where we have only the sum of the input beam charge and the charge of the phase mask.

NPC Fabrication.—We fabricated by electric field poling several spiral and fork shaped NPCs from 0.5 mm thick stoichiometric lithium tantalate with different periods and with different topological charges. The poling periods varied from 10 to 30 μm. The topological charges were $l_c = 1, 5, 20, 50$.

Experimental setup.—A $\hat{\mathbf{y}}$-polarized Nd:YAG Q-switched laser beam ($\lambda = 1.0645$ μm) was directed through a spatial filter and loosely focused by a lens to a 340 μm waist on the twisted NPC (in the transverse configuration). Spectral filters placed after the NPC filtered the pump's radiation and maintained only the SH radiation. A CCD camera, 9 cm after the twisted NPC, captured the output vortex beams.

Results.—In Fig. 3 the experimental profiles (right column) are compared to numerical results computed by a beam propagation method (middle column). The quadratic power dependence shown in Fig. 4(c) confirms that the measured vortex resulted from the nonlinear process. The internal conversion efficiency for the measured average SH vortex excluding Fresnel losses at the crystal facets was $1.35 \times 10^{-7}\%$ (1/W). The mode purity of the generated beam, i.e., the correlation between the theoretical and the measured intensity pattern of Laguerre Gaussian (LG) mode [11], was 83% for the LG_{10} mode, indicating high mode purity.

Nonlinear radius shaping.—One interesting result of the nonlinear generation of vortex beams is the reduction in the vortex's radius. The vortex's radius is measured as the distance from the vortex's (dark) center to the highest intensity ring. When a vortex is diffracted, its radius scales as the square root of the wavelength and topological charge product [1,23], i.e., $R_{\text{vortex}} \propto \sqrt{l\lambda}$. The wavelength of the SH nonlinearly generated vortex is half the pump's wavelength; hence, the diffracted SH vortex's radius is reduced by a factor of $\sqrt{2}$. This is clearly observed in Fig. 4(a). To convert the pump beam into a vortex beam we used the same nonlinear crystal as a linear phase plate. This was enabled by the selective etching of the crystal's facets. The radius scaling property can be used for all optical control of the vortex's radius.

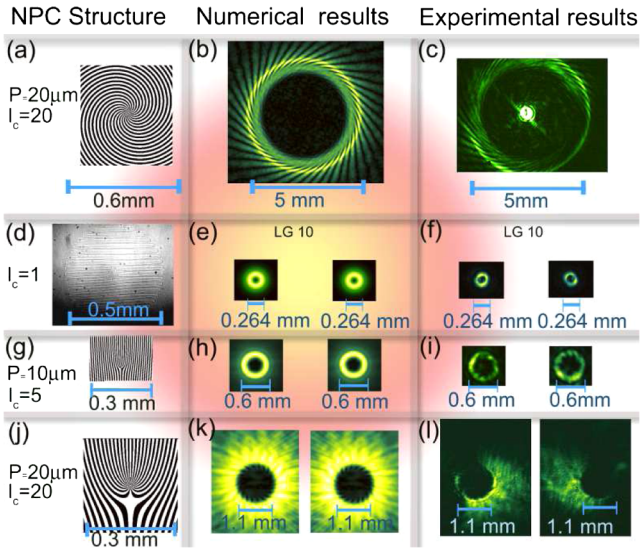

FIG. 3 (color online). Experimental and numerical results of SH vortices generated by twisted NPCs from a TEM_{00} Gaussian pump beam 9 cm from the crystal. (a), (b), (c) Spiral beam generated from the spiral shaped NPC. (d), (e), (f), (g), (h), (i), (j), (k), (l) Vortex beams evolved from fork shaped NPCs with topological charges of $l_c = 1, 5, 20$.

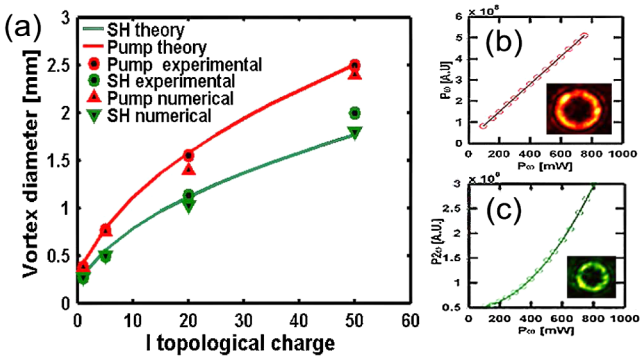

FIG. 4 (color online). Output vortex's radius and power dependence. (a) Theoretical, numerical and experimental results for pump and SH vortices' diameters as a function of topological charge. (b), (c) The power of pump and SH vortices as a function of pump input power.

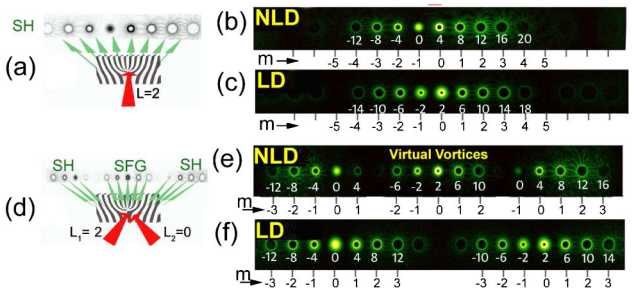

FIG. 5 (color online). Engineering OAM states. Differences between linear and nonlinear diffractions (LD, NLD). $L_c = 4$ in all cases, m denotes the vortex's order, $\lambda_{\text{pumpNLD}} = 1.064\ \mu$m, $\lambda_{\text{inputLD}} = 0.532\ \mu$m. (a) The input OAM is $L = 2$. (b) The OAM of the nonlinear diffracted beam is: $L_{\text{NLD}} = 4 + 4m$. (c) The OAM of the linear diffracted beam is different: $L_{\text{LD}} = 2 + 4m$. (d) Diffraction from two input beams with OAM of $L_1 = 2$, $L_2 = 0$. (e) The nonlinear diffraction of two input beams includes the SH of each beam. In addition, the SFG nonlinear process yields a mutual diffraction, also known as the "virtual beam" effect [25], located at the angle bisector of two beams. This type of diffraction has no analogy in linear optics. The OAM of the "virtual vortices" is $L_{\text{NLD}}(\text{SFG}) = L_1 + L_2 + mL_c$. (f) Linear diffraction of two input beams.

Engineering OAM states.—We studied the differences between the linear and nonlinear diffractions noted in Fig. 5 as LD and NLD respectively. For this purpose, we simulated a 1.0645 μm input pump beam with a topological charge of $l_p = 2$, entering transversely into a fork shaped NPC with a topological charge of $l_c = 4$, as shown in Fig. 5(a). The output SH intensity pattern is presented in Fig. 5(b). We compared this to a linear diffraction of an input beam of 0.532 μm having topological charge of $l_{\text{input}} = 2$ from a fork shaped linear phase mask with a topological charge of $l_c = 4$ as shown in Fig. 5(c). Here, we can clearly observe the difference between linear and nonlinear diffractions. Each process yields a different set of vortices with different topological charges. Another interesting phenomenon which does not occur in a linear diffraction process is caused by the nonlinear mixing of two different beams as depicted in Fig. 5(d). When two noncollinear input beams arrive at an angle to each other, the nonlinear diffraction pattern includes the SH of each of the input beams, as well as a new set of vortices generated by the sum-frequency generation (SFG) nonlinear process [25], as shown in Fig. 5(e). Note that the nonlinear SFG process mixes not only frequencies but also the value of angular momentum. These "virtual vortices" are the outcome of a mutual diffraction process. This is a unique nonlinear phenomenon which is not observed at the linear diffraction of two input beams [Fig. 5(f)]. This enables the generation of multiple vortices having various charges at various diffraction angles. Another possibility is to enhance the shape and polarization properties of the nonlinear generated vortices is by utilizing the Čerenkov nonlinear diffraction (as shown in the Supplemental Material [26]).

Conclusions.—We studied nonlinear interactions in twisted NPCs. We found that the *quasi-angular-momentum* should be included in the general OAM conservation law of nonlinear interactions. The radiation scattered from the twisted NPCs has a new frequency, translational momentum, and angular momentum, enabling the conversion of a nonvortex fundamental beam into a SH vortex beam. Moreover, these crystals mix angular momentum and frequency while adding the topological charge of the crystal to the mixing product. We studied new configurations for engineering various OAM states and proposed a method to enhance the vortices' efficiency using the Čerenkov nonlinear diffraction. These twisted NPCs could give rise to new applications for vortex beams in microparticle manipulation and in the field of quantum information.

This work was partly supported by the Israel Science Foundation and by the Israeli Ministry of Science.

*noavoloch@gmail.com

[1] L. Allen, M. W. Beijersbergen, R. J. C. Spreeuw, and J. P. Woerdman, Phys. Rev. A **45**, 8185 (1992).
[2] J. F. Nye and M. V. Berry, Proc. R. Soc. A **336**, 165 (1974).
[3] A. T. O'Neil, I. MacVicar, L. Allen, and M. J. Padgett, Phys. Rev. Lett. **88**, 053601 (2002).
[4] M. S. Soskin, V. N. Gorshkov, M. V. Vasnetsov, J. T. Malos, and N. R. Heckenberg, Phys. Rev. A **56**, 4064 (1997).
[5] H. He, M. E. J Friese, N. R. Heckenberg, and H. Rubinsztein-Dunlop, Phys. Rev. Lett. **75**, 826 (1995).
[6] A. Mair, A. Vaziri, G. Weihs, and A. Zeilinger, Nature (London) **412**, 313 (2001).
[7] F. Tamburini, B. Thidé, G. M. Terriza, and G. Anzolin, Nature Phys. **7**, 195 (2011).
[8] J. Verbeeck, H. Tian, and P. Schattschneider, Nature (London) **467**, 301 (2010).
[9] T. J. Alexander, Y. S. Kivshar, A. V. Buryak, and R. A. Sammut, Phys. Rev. E **61**, 2042 (2000).
[10] A. S. Desyatnikov, Y. S. Kivshar, and L. Torner, Prog. Opt. **47**, 291 (2005).
[11] J. Courtial, K. Dholakia, L. Allen, and M. J. Padgett, Phys. Rev. A **56**, 4193 (1997).
[12] M. Yamada, N. Nada, M. Saitoh, and K. Watanabe, Appl. Phys. Lett. **62**, 435 (1993).
[13] V. Berger, Phys. Rev. Lett. **81**, 4136 (1998).
[14] I. Freund, Phys. Rev. Lett. **21**, 1404 (1968).
[15] A. Arie and N. Voloch, Laser Photon. Rev. **4**, 355 (2010).
[16] S. M. Saltiel, D. N. Neshev, R. Fischer, W. Krolikowski, A. Arie, and Y. S. Kivshar, Phys. Rev. Lett. **100**, 103902 (2008).
[17] S. M. Saltiel, D. N. Neshev, W. Krolikowski1, A. Arie, O. Bang, and Y. S. Kivshar, Opt. Lett. **34**, 848 (2009).
[18] A. Shapira, R. Shiloh, I. Juwiler, and A. Arie, Opt. Lett. (to be published).
[19] Y. Zhang, J. Wen, S. N. Zhu, and M. Xiao, Phys. Rev. Lett. **104**, 183901 (2010).
[20] A. Bahabad and A. Arie, Opt. Express **15**, 17 619 (2007).

[21] L. Tian, F. Ye, and X. Chen, Opt. Express **19**, 11 591 (2011).
[22] S. M. Saltiel, Y. Sheng, N. Voloch-Bloch, D. N. Neshev, W. Krolikowski, A. Arie, K. Koynov, and Y. S. Kivshar, IEEE J. Quantum Electron. **45**, 1465 (2009).
[23] This dependence is different than that found by [24] probably because the effective aperture in our experiment was large compared to the vortex's scale.
[24] J. E. Curtis and D. G. Grier, Phys. Rev. Lett. **90**, 133901 (2003).
[25] S. M. Saltiel, D. N. Neshev, W. Krolikowski, N. Voloch-Bloch, A. Arie, O. Bang, and Y. S. Kivshar, Phys. Rev. Lett. **104**, 083902 (2010).
[26] See Supplemental Material at http://link.aps.org/supplemental/10.1103/PhysRevLett.108.233902 for longitudinal quasi-phase-matching, transverse nonlinear diffraction, verification of SH vortices, poling process of the crystal, Cerenkov vortex shaping, and the vortex's polarization shaping.